Human Pathology (2019) **91**, 77–85

ELSEVIER

Human PATHOLOGY

www.elsevier.com/locate/humpath

Original contribution

OLIG2 is a marker of the fusion protein-driven neurodevelopmental transcriptional signature in alveolar rhabdomyosarcoma☆

Shyam S. Raghavan MD[a], Kelly L. Mooney MD[a], Andrew L. Folpe MD[b], Gregory W. Charville MD, PhD[a,*]

[a]*Department of Pathology, Stanford University School of Medicine, Stanford, California 94305, USA*
[b]*Department of Laboratory Medicine and Pathology, Mayo Clinic, Rochester, MN 55905, USA*

Received 9 June 2019; accepted 3 July 2019

Keywords:
Rhabdomyosarcoma;
PAX3;
PAX7;
Translocation;
Immunohistochemistry;
Gene expression;
OLIG2

Summary Alveolar rhabdomyosarcoma (RMS) is associated with an underlying pathogenic translocation involving either *PAX3* or *PAX7* and *FOXO1*. The presence or absence of this fusion defines the biology and clinical behavior of this subtype of RMS and its identification in tumors is relevant to prognostication and treatment planning. To further explore the unique characteristics of fusion-driven RMS, we leveraged a published gene expression data set to perform an unbiased comparison of 33 fusion-positive and 25 fusion-negative RMS cases. Our analyses revealed 1790 expressed loci with more than two-fold differential expression at a threshold of $P < .05$. Genes with increased expression in fusion-positive relative to fusion-negative RMS were significantly enriched for those involved in "nervous system development," "neuron differentiation," and "neurogenesis," highlighting a neurodevelopmental gene expression signature driven by the alveolar RMS-associated fusion protein. We show that neurodevelopmental genes are enriched near PAX3-FOXO1 fusion protein binding sites, suggesting a genome-wide fusion protein-mediated activation of *cis* regulatory elements. Among the genes with differential expression in fusion-positive versus fusion-negative RMS, we identified expression of the transcriptional regulator of motor neuron and oligodendrocyte development, *OLIG2*, as a marker of the fusion protein-dependent neurodevelopmental signature. Immunohistochemical analysis of a cohort of 73 RMS specimens revealed OLIG2 expression in 96.4% of fusion-positive RMS (N = 27/28), but only in 6.7% of fusion-negative RMS (N = 3/45; $P < .001$). The proportion of OLIG2-expressing cells in fusion-negative cases did not exceed 5%, while 92.9% of fusion-positive cases showed expression in at least 5% of cells. Our findings identify OLIG2 expression as a unique manifestation of a neurodevelopmental gene expression signature driven by the oncogenic fusion protein characteristic of alveolar RMS, which may aid in the diagnostic and prognostic distinction of fusion-positive cases.

☆ **Funding:** The authors received no financial support for the research, authorship, and/or publication of this article. **Declaration of conflicting interests:** The authors declare no potential conflicts of interest with respect to the research, authorship, and/or publication of this article.

* Corresponding author at: Department of Pathology, Stanford University School of Medicine, 300 Pasteur Drive, Lane 235, Stanford, CA 94305-5324.
E-mail address: gwc@stanford.edu (G. W. Charville).

https://doi.org/10.1016/j.humpath.2019.07.003
0046-8177/

1. Introduction

Rhabdomyosarcoma (RMS) is subdivided into alveolar, embryonal, pleomorphic, and spindle cell/sclerosing subtypes [1]. Since these subtypes of RMS differ considerably with regard to prognosis and treatment, their diagnostic distinction is often clinically significant. Characterized histologically by the presence of discohesive round cells arranged in nests encircled by fibrovascular septa mimicking the microscopic architecture of lung parenchyma (Fig. 1A), the alveolar subtype is uniquely associated with a recurrent pathogenic translocation involving the 5′ terminus of *PAX3*, or, less commonly, *PAX7*, and the 3′ end of *FOXO1* [2-4].

Although alveolar morphology generally coincides with the presence of an underlying PAX3/7-FOXO1 fusion protein, a subset of alveolar-appearing tumors will be fusion-negative (Fig. 1B). Importantly, these fusion protein-negative RMS cases with an alveolar-type growth pattern are indistinguishable from embryonal RMS in terms of their gene expression characteristics, whole-chromosome copy number changes, and clinical behavior [5,6]. Because accurate risk stratification is required for treatment planning in RMS, recent clinical trials (i.e., Children's Oncology Group study ARST1431) have classified RMS subtypes using fusion status rather than histology.

The presence of *FOXO1* gene rearrangement in RMS is often detected using traditional cytogenetics or fluorescence in situ hybridization (FISH). The more recent advent of next generation sequencing-based approaches has enabled identification of pathogenic *PAX3/7-FOXO1* translocations in the context of broader genomic characterizations of RMS. In parallel to these techniques, immunohistochemical analysis of gene expression changes as a surrogate of an underlying pathogenic fusion protein has emerged as an important approach to the diagnosis of several other soft tissue entities. Such analyses generally take one of two forms. A component of the fusion protein itself (often over-expressed in translocation-driven tumors) can be detected, as is the case for FLI1 and ERG in Ewing sarcoma or STAT6 in solitary fibrous tumor [7-10]. Alternatively, a distinct transcriptional target of the fusion protein (or combination of targets) can be analyzed for expression by immunohistochemistry or in situ hybridization – examples include NKX2.2 and PAX7 in Ewing sarcoma, or E26 transformation-specific (ETS) transcription factors in *CIC*-rearranged sarcoma [11-19].

Several studies to date have examined gene expression differences in fusion-driven RMS as compared to its fusion-negative counterpart. Although the large majority of fusion-negative RMS expresses some amount of myogenin, strong and diffuse expression of myogenin is closely associated with the presence of *PAX3/7-FOXO1* translocations [20-22]. Conversely, expression of PAX7 is typically limited in fusion-positive RMS, although the heterogeneity of PAX7 expression in fusion-negative cases limits the utility of this immunohistochemical pattern in determining underlying fusion status [23]. Genome-wide expression profiling using oligonucleotide microarrays has clearly demonstrated that the sum of gene expression dynamics across hundreds of genetic loci can reliably distinguish tumors bearing the *PAX3/7-FOXO1* translocation from those without it, including morphologically alveolar-appearing fusion-negative cases [24,25]. Such studies have also pointed to specific proteins, such as AP2β and

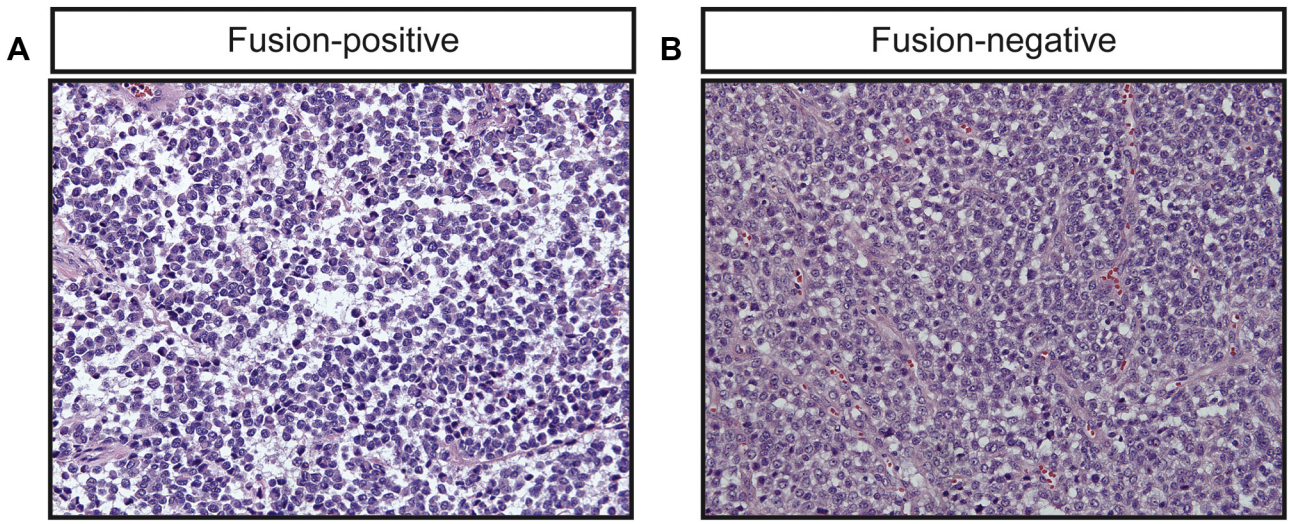

Fig. 1 Morphologic similarities of fusion-positive and fusion-negative rhabdomyosarcoma. Fusion-positive A, and fusion-negative B, rhabdomyosarcoma can be morphologically indistinct. Representative H&E-stained histologic sections of fusion-positive rhabdomyosarcoma (A) and fusion-negative rhabdomyosarcoma (B) at 200× magnification demonstrates examples with similar morphologic appearance, characterized by primitive-appearing, discohesive, round cells with fairly inconspicuous thin-walled vessels and a lack of significant matrix production in the background.

HMGA2, with biased expression in fusion-positive and -negative cases, respectively, that can be detected using immunohistochemistry [22,26]. Despite these insights, there is still much to be learned about the effects of the *PAX3/7-FOXO1* translocation on the gene expression program of RMS, the mechanistic significance of these transcriptional changes specifically with regard to fusion gene-related clinical prognosis, and the diagnostic utility of analyzing specific *PAX3/7-FOXO1* target genes in RMS cases.

A particularly unexpected feature of the fusion protein-associated transcriptional signature is overexpression of genes linked to nervous system development. While some gene expression analyses of RMS have noted enrichment for neural-related genes in the fusion protein signature, others have not [24,25,27,28]. Therefore, it is unclear whether this neurodevelopmental gene expression signature represents a consistent and diagnostically useful characteristic of fusion-driven RMS. Moreover, there is not yet a mechanistic accounting for neural gene expression in alveolar RMS. In particular, we do not know whether neurodevelopmental genes expressed in alveolar RMS are directly bound by the fusion protein itself. Of even more practical significance, the specific genes that comprise this signature have not been fully explored. Therefore, the extent to which the expression of individual genes can be assessed routinely as a surrogate marker of the fusion protein remains unknown.

In this context, we aimed to study publicly available gene expression data from fusion gene-positive and -negative RMS in order to better understand the function of the fusion protein in regulating transcriptional programs linked to specific signaling pathways and developmental programs. Our observations affirm a unique link between fusion-driven rhabdomyosarcoma and neurodevelopmental transcriptional hierarchies, implicate specific elements of these hierarchies that are amenable to diagnostic interrogation by immunohistochemistry, and ultimately provide a framework for similar characterizations of gene expression regimes in other translocation-driven sarcomas.

2. Materials and methods

2.1. Cases

Cases of RMS were retrospectively retrieved from the archives of Stanford Medical Center under an Institutional Review Board-approved protocol. The presence of *FOXO1* gene rearrangement was evaluated in all specimens by either (1) interphase fluorescence in situ hybridization (FISH) using the Vysis break-apart probes (Abbott Laboratories, Abbott Park, IL), or (2) karyotype characterization by metaphase chromosome analysis of disaggregated tumor biopsies in short-term culture using G-banding (GTW method). The study cohort for OLIG2 immunohistochemistry included 73 RMS cases altogether (45 fusion-negative and 28 fusion-positive). Fusion-negative cases included 33 embryonal, 7 pleomorphic, and 5 spindle cell/sclerosing RMS.

2.2. Immunohistochemistry

Immunohistochemical detection of OLIG2 and desmin was performed essentially as previously described [7,23]. After antigen retrieval, histologic sections were stained with antibodies according to standard protocols for formalin-fixed, paraffin-embedded material. A monoclonal antibody against OLIG2 raised in mouse (Clone 211F1.1) was purchased from Cell Marque (Rocklin, CA). Anti-OLIG2 antibody was used at a dilution of 1:100 (by volume) following antigen retrieval using Leica Epitope Retrieval Solution 2 on the Leica BOND platform. Anti-OLIG2 immunoreactivity was assessed as a percentage of neoplastic cells exhibiting nuclear-localized chromogen using a single, whole representative histologic section of tumor. Tumors were considered positive for OLIG2 expression if more than 1% of neoplastic cells exhibited anti-OLIG2 immunoreactivity.

A monoclonal antibody against myogenin (clone F5D) raised in mouse was purchased from Agilent-Dako (Santa Clara, CA) and used at a dilution of 1:200 (by volume). All cases of fusion-positive RMS exhibited characteristic diffuse myogenin expression by immunohistochemistry. Myogenin expression in fusion-negative cases was more heterogeneous, ranging from focal to diffuse among the fusion-negative cases used in this study.

2.3. Gene expression analysis

Publically available microarray and chromatin immunoprecipitation-sequencing (ChIP-seq) data were accessed via the Gene Expression Omnibus (GEO) between September 15, 2017, and July 20, 2018. Microarray data (GSE66533) [29] were analyzed using the Partek Genomics Suite (version 6.6) with inclusion of all specimens after sample quality and principal component analyses.

The DAVID bioinformatics database functional annotation tool was used for gene-set enrichment analyses on expression-defined subsets [30]. Statistical analyses of overlap between gene lists were performed using a hypergeometric probability test, invoking a population size of 26 292 in evaluations of human gene sets. For comparisons of individual gene microarray data expression values, normality was first characterized using a Shapiro-Wilk test; a Mann-Whitney rank sum test was used to evaluate differences between groups of non-normal data, while a Student *t* test was used to evaluate differences between groups of normal data. A two-proportion Z-test was employed to compare the percentage of RMS cases positive for OLIG2 expression by immunohistochemistry.

Employing the DAVID bioinformatics suite, *UCSC_TFBS* analysis was performed on all differentially expressed genes in fusion-positive versus -negative RMS to predict the transcription factors regulating these genes. $P < .05$ was used as the

threshold for inclusion of transcription factors in the regulatory network. Using the identified transcription factors as nodes, we constructed a network based on known interactions among transcription factors using STRING version 9.05 [31]. Disconnected nodes were excluded from the network.

3. Results

To explore differential gene expression in fusion-positive and fusion-negative RMS, we first performed analyses of microarray-based genome-wide gene expression data from 33 fusion-positive and 25 fusion-negative samples (GEO data series GSE66533) [29]. Among 54 675 analyzed genetic loci, we identified 1790 transcripts showing differential expression between fusion gene-positive and -negative cases, using a fold-change of greater than two and a false discovery rate (FDR) of less than 0.05 to define significantly differential expression (Fig. 2A). Hierarchical clustering of the 58 RMS cases based on expression levels in these 1790 probe-sets enabled separation of all samples according to fusion gene status (Fig. 2A), indicating that the summation of these probe-sets results in a fusion-related transcriptional signature.

To further characterize the gene expression differences present in fusion-positive versus -negative RMS, we performed gene-set enrichment analyses of the aforementioned differentially expressed loci (Fig. 2B). Among 595 annotated genes with greater than two-fold increased expression in fusion-positive cases relative to fusion-negative, there were 116 genes associated with "nervous system development" (GO:0007399; $P = 2.0 \times 10^{-12}$). Related gene-sets, including those associated with "generation of neurons" (GO:0048699; 82 genes; $P = 2.9 \times 10^{-11}$), "neuron differentiation" (GO:0030182; 75 genes; $P = 1.5 \times 10^{-10}$), and "neurogenesis" (GO:0022008; 83 genes; $P = 2.8 \times 10^{-10}$), were similarly enriched. Genes with greater than two-fold increased expression in fusion-positive RMS also included those associated with "muscle structure development" (GO:0061061; 46 genes; $P = 7.7 \times 10^{-10}$) and "striated muscle tissue development" (GO:0014706; 33 genes; $P = 3.6 \times 10^{-9}$), although the number of genes associated with these ontologies was exceeded by those associated with neurodevelopmental signatures.

Given the association of this neurodevelopmental gene expression signature with the presence of the oncogenic fusion protein in RMS, we hypothesized that the fusion protein itself was at least partly responsible for the transcriptional activation of this unique subset of genes. To test this hypothesis, we first constructed a transcription factor regulatory network of neurodevelopmental genes expressed in fusion-positive RMS (Fig. 3A). Briefly, our analysis identified transcription factors with predicted binding sites enriched among the gene list and generated a network of these transcription factors based on a curated database of protein–protein interactions (see Materials and Methods). Interestingly, this unbiased approach generated a transcriptional regulatory network with nodes that included

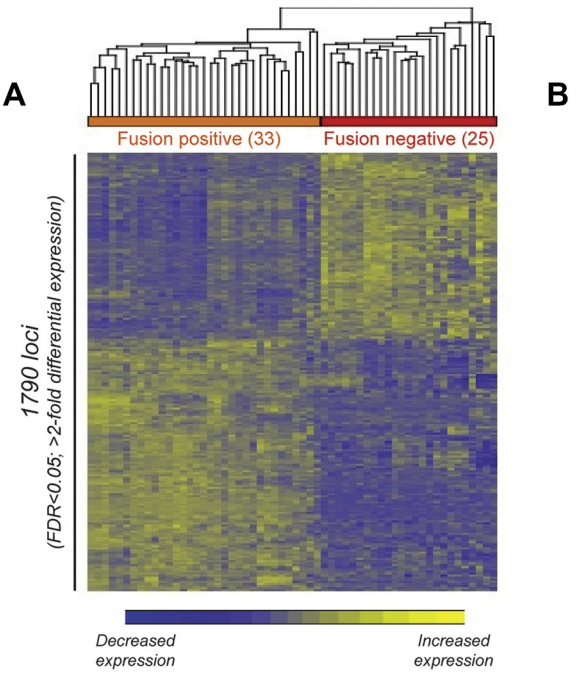

B

GO Term	P-value	Gene count
Cell development	3.8×10^{-14}	113
Nervous system development	2.0×10^{-12}	116
Regulation of cell differentiation	6.6×10^{-12}	91
Generation of neurons	2.9×10^{-11}	82
Neuron differentiation	1.5×10^{-10}	75
Positive regulation of developmental process	2.2×10^{-10}	69
Neurogenesis	2.8×10^{-10}	83
Positive regulation of cell differentiation	3.7×10^{-10}	58
Muscle structure development	7.7×10^{-10}	46
Regulation of multicellular organismal development	8.9×10^{-10}	92

Fig. 2 Comparison of gene expression in fusion-positive versus fusion-negative rhabdomyosarcoma. A, Heat-map of differentially expressed genes in fusion-positive versus fusion-negative rhabdomyosarcoma. Thirty-three fusion-positive sarcomas and 25 fusion-negative were clustered according to microarray-based gene expression signatures [29]. B, List of the 10 annotated gene ontology (GO) terms associated with genes enriched with the lowest *P*-values among genetic loci overexpressed in fusion-positive versus fusion-negative rhabdomyosarcoma. Terms associated with neurodevelopmental gene expression are highlighted in red.

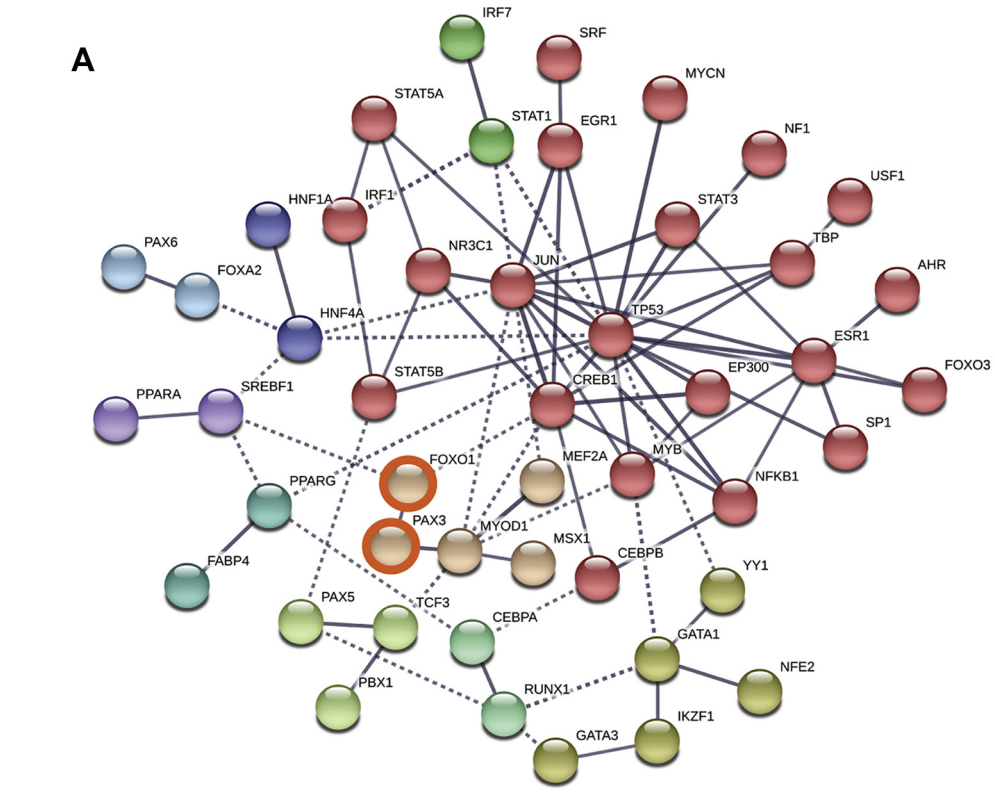

GO Term	P-value	Gene count
Cell development	4.2×10^{-14}	140
Embryo development	1.6×10^{-13}	85
Regulation of cell differentiation	4.4×10^{-12}	113
Nervous system development	7.6×10^{-12}	143
Regulation of multicellular organismal development	1.9×10^{-11}	120
Anatomic structure formation involved in morphogenesis	3.8×10^{-11}	90
Chordate embryonic development	6.5×10^{-11}	57
Generation of neurons	7.2×10^{-11}	100
Neurogenesis	1.1×10^{-10}	104
Embryonic morphogenesis	1.3×10^{-10}	56

Fig. 3 PAX3-FOXO1 directs a neurogenic gene expression program in fusion-positive rhabdomyosarcoma. A, Transcription factor regulatory network of the neurodevelopmental gene expression program from analysis of differential gene expression in fusion-positive and -negative rhabdomyosarcoma. PAX3 and FOXO1 are highlighted in orange. B, Overlap between PAX3-FOXO1-bound genes and those genes with increased expression in fusion-positive rhabdomyosarcoma. C, List of the 10 annotated gene ontology (GO) terms associated with genes bound by PAX3-FOXO1 in rhabdomyosarcoma. Terms associated with neurodevelopmental gene expression are highlighted in red.

both FOXO1 ($P = 5.8 \times 10^{-10}$) and PAX3 ($P = 2.8 \times 10^{-8}$), suggesting a predicted role for the translocation protein in this distinct signature of neuronal genes.

Previous studies of the PAX3-FOXO1 fusion protein using chromatin immunoprecipitation combined with DNA sequencing (ChIP-seq) have identified genome-wide binding

sites of the translocation protein product [32]. In order to understand the contribution of PAX3-FOXO1 to the transcriptional activation of genes in fusion-positive RMS, we asked whether genes overexpressed in fusion-positive relative to fusion-negative RMS coincided with those genes adjacent to PAX3-FOXO1 binding sites. Notably, 139 of the 689 annotated genes identified by nearby PAX3-FOXO1 binding sites were also overexpressed in fusion-positive RMS (Fig. 3B; $P = 4.6 \times 10^{-92}$), suggesting that proximity of fusion protein binding is functionally relevant to locus-specific transcriptional activation. Furthermore, the 689 PAX3-FOXO1-bound genes themselves were significantly enriched for those involved in "nervous system development" (143 genes; $P = 7.6 \times 10^{-12}$), "generation of neurons" (100 genes; $P = 7.2 \times 10^{-11}$), and "neurogenesis" (Fig. 3C; 104 genes; $P = 1.1 \times 10^{-10}$). Altogether, 35 genes associated with nervous system development were overexpressed in fusion-positive RMS and bound by the fusion protein. These findings point to a fusion-protein-regulated transcriptional program that is characterized by expression of neurodevelopmental genes.

Next, we analyzed specific neurodevelopmental genes transcriptionally regulated by PAX3-FOXO1 as potential biomarkers of the fusion protein. Among neurodevelopmental genes that are both overexpressed in fusion-positive RMS and bound by PAX3-FOXO1 itself, we identified eight encoding transcription factors, including *SOX8*, *ATOH8*, *FOXP1*, *PAX3*, *PROX1*, *TFAP2B* (encoding AP2β), *MYCN*, and *OLIG2*. We focused on transcription factors given both that they often exhibit robust expression as master regulators overseeing broad networks of expressed genes and that their nuclear localization is readily amenable to immunohistochemical interrogation. Of these eight genes, *OLIG2* showed the most significant differential expression in fusion-positive RMS relative to fusion-negative RMS (Fig. 4A; 18.5-fold differential expression; $P = 1.1 \times 10^{-21}$). Taking together all 54 675 analyzed genetic loci, *OLIG2* was the sixteenth most differentially expressed locus in microarray comparisons of fusion-positive and fusion-negative cases. Expression of myogenic regulatory factors is the sine qua non of RMS diagnosis; the relative expression of MYOG, being more diffuse in fusion-positive RMS, is a marker of the alveolar subtype [33]. The relative overexpression of *OLIG2* (18.5-fold) in fusion-positive cases exceeded that of both *MYOG* (2.7-fold) and *MYOD1* (2.4-fold) by analysis of published microarray data (Fig. 4B). Moreover, the pattern of expression of *OLIG2* was the inverse of that of *PAX7* (Fig. 4B), a marker of myogenic differentiation that is more diffusely expressed in the majority of embryonal RMS relative to its more limited expression in alveolar RMS [23]. Thus, *OLIG2* expression is a characteristic of the fusion-positive (i.e., alveolar) subtype of RMS.

To further explore the diagnostic significance of this neurodevelopmental gene signature, and of *OLIG2* expression in particular, in the distinction of fusion-positive and fusion-negative RMS, we used immunohistochemistry to detect OLIG2 protein in a cohort of RMS cases that have been characterized with regard to *FOXO1* rearrangement. Full histologic cross sections of tumor were evaluated microscopically. OLIG2 is a transcription factor and anti-OLIG2 immunoreactivity was consistently localized to the nucleus (Fig. 5A) with little or no cytoplasmic staining. While OLIG2 expression was detected by immunohistochemistry in 96.4% (N = 27/28) of fusion-positive RMS, only 6.7% (N = 3/45) of fusion-negative RMS expressed any OLIG2 ($P < .001$; Fig. 5B).

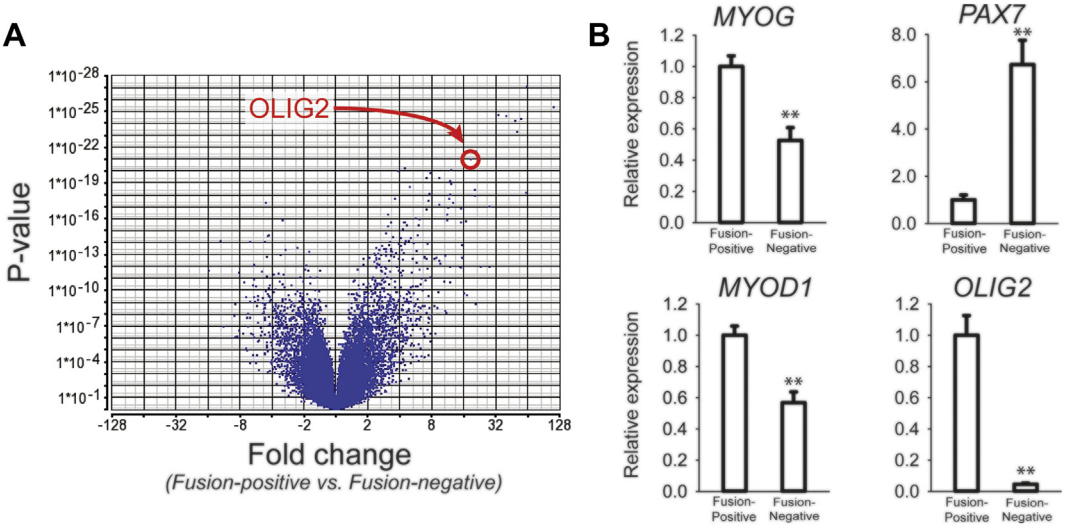

Fig. 4 OLIG2 is a neurodevelopmental transcription factor showing relative overexpression in fusion-positive rhabdomyosarcoma. A, Volcano plot showing *P* value versus fold-change in a comparison of high-throughput microarray gene expression data from 33 fusion-positive and 25 fusion-negative rhabdomyosarcoma samples [29]. Each point on the plot represents one of 54 675 individually analyzed loci. *OLIG2* is highlighted as a gene with significantly enriched expression in fusion-positive rhabdomyosarcoma relative to fusion-negative. B, Relative expression of selected genes by gene expression microarray analysis. Expression values are normalized to 1.0 in fusion-positive cases. Error bars represent standard error of the mean. (**$P < .001$).

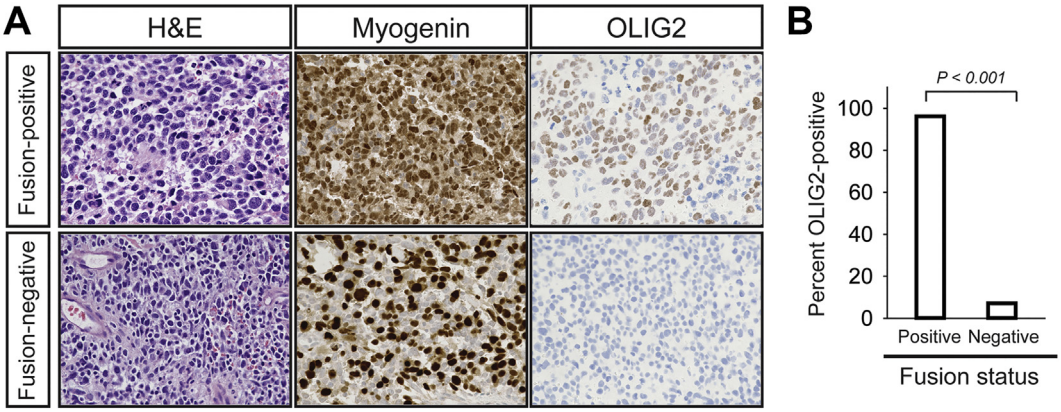

Fig. 5 Immunohistochemical analysis of OLIG2 expression in rhabdomyosarcoma. A, Representative immunohistochemical detection of OLIG2 expression in fusion-positive and -negative rhabdomyosarcoma, both of which are characterized by strong and diffuse expression of myogenin. B, Percentage of fusion-positive and -negative rhabdomyosarcoma cases showing OLIG2 expression by immunohistochemistry.

Moreover, OLIG2 expression in fusion-negative cases was not seen in more than 5% of lesional cells, while 92.9% (N = 26/28) of fusion-positive cases expressed OLIG2 in more than 5% of cells. On average, 49% of cells expressed OLIG2 in fusion-positive cases. Among the fusion-positive cohort, the 5′ partner of the FOXO1 translocation was identified in 15 cases (13 *PAX3-FOXO1* and 2 *PAX7-FOXO1*), all of which were OLIG2-positive. In addition to 33 cases of embryonal RMS, including 3 with limited OLIG2 expression, fusion-negative cases included 7 examples of pleomorphic RMS and 5 of spindle cell/sclerosing RMS, all of which were negative for OLIG2 expression. Therefore, immunohistochemical detection of OLIG2 expression reflects a neurodevelopmental gene expression signature characteristic of fusion-positive RMS.

4. Discussion

RMS is characterized by expression of markers of skeletal muscle differentiation, including MYOD1 and myogenin. In our study, comparisons of genome-wide gene expression in fusion protein-positive and -negative RMS highlighted enriched expression of neurodevelopmental-related genes in fusion-positive cases. These findings may relate to the previously reported diagnostic pitfall of synaptophysin or chromogranin expression in as much as 43% of morphologically defined alveolar RMS cases [34]. CD56 is almost always expressed in RMS, although CD56 expression in isolation is not necessarily interpreted as indicative of neuroendocrine differentiation in RMS. In contrast to this previous study of neuroendocrine marker expression in alveolar RMS, our study identified more pervasive expression of a neurodevelopmental gene signature, as represented by the transcription factor OLIG2 (~96% positive in *FOXO1*-rearranged RMS cases). Additionally, previous examination of neuroendocrine marker expression in alveolar RMS did not include a comparison to embryonal/fusion-negative RMS, so it remains unclear whether features of neuroendocrine differentiation in particular distinguish the fusion-positive subtype. Anecdotally, we have not observed significant expression of neuroendocrine markers in RMS cases of embryonal, pleomorphic, or spindle cell/sclerosing subtypes in our own practices.

Our analyses identified OLIG2 expression as a feature of the neurodevelopmental cell phenotype that manifests in fusion-positive rhabdomyosarcoma. We find that *OLIG2* is representative of a broader fusion protein-related neurodevelopmental gene expression signature that includes “neural-related” genes such as *ANK2*, *NRCAM*, *KCNN3*, and *DCX*, noted to exhibit *PAX3/7-FOXO1*-related overexpression in previous studies [24,25]. OLIG2 is a basic helix–loop–helix transcription factor that is required, along with OLIG1, for appropriate development of motor neurons and oligodendrocytes in mice [35]. Accordingly, OLIG2 is expressed in ventral neural progenitor cells that differentiate into oligodendrocytes and subsets of neurons in the brain and spinal cord. Previous studies have shown that OLIG2 is also expressed in 97% of glial neoplasms, including oligodendroglioma, astrocytoma, and ependymoma [36]. Moreover, OLIG2 is expressed in the large majority of “neuronal neoplasms”, such as medulloblastoma, central neurocytoma, and dysembryoplastic neuroepithelial tumor [36]. Although previous studies have suggested that OLIG2 is “not expressed in non-neuroectodermally derived tumors” [36], these analyses did not examine expression in RMS or other soft tissue sarcomas.

A single case used in this study classified as alveolar RMS showed no evidence of OLIG2 expression. This RMS presented as a soft tissue mass of the posterior lower leg in a 10 year-old female with a history of acute promyelocytic leukemia post bone marrow transplant. The tumor was classified on the basis of alveolar morphology, expression of myogenin, and apparent *FOXO1* rearrangement by interphase FISH (separation of 5′ and 3′ probes in 79% of cells in this break-apart assay). Concurrent chromosomal analysis of this tumor after short-term culture revealed a subset of cells with an apparent chromosome #13 long arm

deletion. Sequential metaphase FISH analysis demonstrated complete loss of the *FOXO1* locus from the putative del (13q), consistent with chromosomal deletion, rather than a t (2;13) or t(1;13) derivative. Although the chromosome 13 deletion was ultimately felt to represent an artifact of culture, it does raise the possibility that the observed FOXO1 rearrangement is mediated by a complex cytogenetic abnormality not necessarily representing a translocation involving *PAX3* or *PAX7*.

As a transcription factor expressed in many neuronal and glial neoplasms of the central nervous system, OLIG2 regulates tumor proliferation [37]. In murine models of glioma, Olig2 activates expression of genes involved in cell-cycle progression, while conditional loss of *Olig2* decreases the rate of tumor growth and prolongs survival [38]. OLIG2 function seems to be particularly important in maintaining a subpopulation of tumor-propagating glioma stem-like progenitor cells [38,39]. The growth-promoting effects of OLIG2 in glioma include modulation of epidermal growth factor receptor (EGFR) and platelet-derived growth factor receptor-α (PDGFRα), both of which are susceptible to pharmaceutical inhibition [38,39]. The observation of OLIG2 expression in this study thus raises the possibility that it mediates similar oncogenic mechanisms in fusion-positive RMS that could be explored as therapeutic targets.

Fusion-positive RMS cases in this study were heterogeneous in terms of the percentage of cells positive for expression of OLIG2. This heterogeneity did not appear to correlate with the age of the specimen or the duration of fixation. An intriguing possibility is that differences in OLIG2 expression between cases somehow reflects differences in the underlying biology of these tumors that may relate to their tissue of origin, degree of differentiation, susceptibility to treatment, and clinical prognosis. Also, individual tumor cells within a given specimen exhibited varying intensities of anti-OLIG2 immunoreactivity. Thus, even within a tumor, factors such as cell-cycle stage, microenvironmental cues, and states of differentiation may manifest with distinct OLIG2 expression in individual cells.

References

[1] Kashi VP, Hatley ME, Galindo RL. Probing for a deeper understanding of rhabdomyosarcoma: insights from complementary model systems. Nat Rev Cancer 2015;15:426-39.

[2] Shapiro DN, Sublett JE, Li B, et al. Fusion of PAX3 to a member of the forkhead family of transcription factors in human alveolar rhabdomyosarcoma. Cancer Res 1993;53:5108-12.

[3] Davis RJ, D'Cruz CM, Lovell MA, et al. Fusion of PAX7 to FKHR by the variant t(1;13)(p36;q14) translocation in alveolar rhabdomyosarcoma. Cancer Res 1994;54:2869-72.

[4] Galili N, Davis RJ, Fredericks WJ, et al. Fusion of a fork head domain gene to PAX3 in the solid tumour alveolar rhabdomyosarcoma. Nat Genet 1993;5:230-5.

[5] Williamson D, Missiaglia E, de Reyniès A, et al. Fusion gene-negative alveolar rhabdomyosarcoma is clinically and molecularly indistinguishable from embryonal rhabdomyosarcoma. J Clin Oncol 2010;28:2151-8.

[6] Skapek SX, Anderson J, Barr FG, et al. PAX-FOXO1 fusion status drives unfavorable outcome for children with rhabdomyosarcoma: a children's oncology group report. Pediatr Blood Cancer 2013;60:1411-7.

[7] Wang W-L, Patel NR, Caragea M, et al. Expression of ERG, an Ets family transcription factor, identifies ERG-rearranged Ewing sarcoma. Mod Pathol 2012;25:1378-83.

[8] Folpe AL, Hill CE, Parham DM, et al. Immunohistochemical detection of FLI-1 protein expression: a study of 132 round cell tumors with emphasis on CD99-positive mimics of Ewing's sarcoma/primitive neuroectodermal tumor. Am J Surg Pathol 2000;24:1657-62.

[9] Rossi S, Orvieto E, Furlanetto A, et al. Utility of the immunohistochemical detection of FLI-1 expression in round cell and vascular neoplasm using a monoclonal antibody. Mod Pathol 2004;17:547-52.

[10] Llombart-Bosch A, Navarro S. Immunohistochemical detection of EWS and FLI-1 proteinss in Ewing sarcoma and primitive neuroectodermal tumors: comparative analysis with CD99 (MIC-2) expression. Appl Immunohistochem Mol Morphol AIMM 2001;9:255-60.

[11] Charville GW, Wang W-L, Ingram DR, et al. EWSR1 fusion proteins mediate PAX7 expression in Ewing sarcoma. Mod Pathol 2017;30:1312-20.

[12] Hung YP, Fletcher CDM, Hornick JL. Evaluation of NKX2-2 expression in round cell sarcomas and other tumors with EWSR1 rearrangement: imperfect specificity for Ewing sarcoma. Mod Pathol 2016;29:370-80.

[13] Yoshida A, Sekine S, Tsuta K, et al. NKX2.2 is a useful immunohistochemical marker for Ewing sarcoma. Am J Surg Pathol 2012;36:993-9.

[14] Toki S, Wakai S, Sekimizu M, et al. PAX7 immunohistochemical evaluation of Ewing sarcoma and other small round cell tumours. Histopathology 2018;73:645-52.

[15] Le Guellec S, Velasco V, Pérot G, et al. ETV4 is a useful marker for the diagnosis of CIC-rearranged undifferentiated round-cell sarcomas: a study of 127 cases including mimicking lesions. Mod Pathol 2016;29:1523-31.

[16] Hung YP, Fletcher CD, Hornick JL. Evaluation of ETV4 and WT1 expression in CIC-rearranged sarcomas and histologic mimics. Mod Pathol 2016;29:1324-34.

[17] Specht K, Sung Y-S, Zhang L, et al. Distinct transcriptional signature and immunoprofile of CIC-DUX4 fusion-positive round cell tumors compared to EWSR1-rearranged Ewing sarcomas: further evidence toward distinct pathologic entities. Genes Chromosomes Cancer 2014;53:622-33.

[18] Smith SC, Palanisamy N, Martin E, et al. The utility of ETV1, ETV4 and ETV5 RNA in-situ hybridization in the diagnosis of CIC-DUX sarcomas. Histopathology 2017;70:657-63.

[19] Smith SC, Buehler D, Choi E-YK, et al. CIC-DUX sarcomas demonstrate frequent MYC amplification and ETS-family transcription factor expression. Mod Pathol Off J U S Can Acad Pathol Inc 2015;28:57-68.

[20] Dias P, Chen B, Dilday B, et al. Strong immunostaining for myogenin in rhabdomyosarcoma is significantly associated with tumors of the alveolar subclass. Am J Pathol 2000;156:399-408.

[21] Hostein I, Andraud-Fregeville M, Guillou L, et al. Rhabdomyosarcoma: value of myogenin expression analysis and molecular testing in diagnosing the alveolar subtype: an analysis of 109 paraffin-embedded specimens. Cancer 2004;101:2817-24.

[22] Rudzinski ER, Anderson JR, Lyden ER, et al. Myogenin, AP2β, NOS-1, and HMGA2 are surrogate markers of fusion status in rhabdomyosarcoma: a report from the soft tissue sarcoma committee of the children's oncology group. Am J Surg Pathol 2014;38:654-9.

[23] Charville GW, Varma S, Forgó E, et al. PAX7 expression in rhabdomyosarcoma, related soft tissue tumors, and small round blue cell neoplasms. Am J Surg Pathol 2016;40:1305-15.

[24] Laé M, Ahn E, Mercado G, et al. Global gene expression profiling of PAX-FKHR fusion-positive alveolar and PAX-FKHR fusion-negative embryonal rhabdomyosarcomas. J Pathol 2007;212:143-51.
[25] Davicioni E, Finckenstein FG, Shahbazian V, et al. Identification of a PAX-FKHR gene expression signature that defines molecular classes and determines the prognosis of alveolar rhabdomyosarcomas. Cancer Res 2006;66:6936-46.
[26] Davicioni E, Anderson MJ, Finckenstein FG, et al. Molecular classification of rhabdomyosarcoma—genotypic and phenotypic determinants of diagnosis: a report from the Children's oncology group. Am J Pathol 2009;174:550-64.
[27] Wachtel M, Schäfer BW. PAX3-FOXO1: zooming in on an "undruggable" target. Semin Cancer Biol 2018;50:115-23.
[28] Ebauer M, Wachtel M, Niggli FK, et al. Comparative expression profiling identifies an in vivo target gene signature with TFAP2B as a mediator of the survival function of PAX3/FKHR. Oncogene 2007;26:7267-81.
[29] Sun W, Chatterjee B, Wang Y, et al. Distinct methylation profiles characterize fusion-positive and fusion-negative rhabdomyosarcoma. Mod Pathol 2015;28:1214-24.
[30] Huang DW, Sherman BT, Lempicki RA. Systematic and integrative analysis of large gene lists using DAVID bioinformatics resources. Nat Protoc 2009;4:44-57.
[31] Franceschini A, Szklarczyk D, Frankild S, et al. STRING v9.1: protein-protein interaction networks, with increased coverage and integration. Nucleic Acids Res 2013;41:D808-15.
[32] Gryder BE, Yohe ME, Chou H-C, et al. PAX3-FOXO1 establishes myogenic super enhancers and confers BET Bromodomain vulnerability. Cancer Discov 2017;7:884-99.
[33] Kumar S, Perlman E, Harris CA, et al. Myogenin is a specific marker for rhabdomyosarcoma: an immunohistochemical study in paraffin-embedded tissues. Mod Pathol 2000;13:988-93.
[34] Bahrami A, Gown AM, Baird GS, et al. Aberrant expression of epithelial and neuroendocrine markers in alveolar rhabdomyosarcoma: a potentially serious diagnostic pitfall. Mod Pathol Off J U S Can Acad Pathol Inc 2008;21:795-806.
[35] Zhou Q, Anderson DJ. The bHLH transcription factors OLIG2 and OLIG1 couple neuronal and glial subtype specification. Cell 2002;109:61-73.
[36] Ligon KL, Alberta JA, Kho AT, et al. The Oligodendroglial lineage marker OLIG2 is universally expressed in diffuse gliomas. J Neuropathol Exp Neurol 2004;63:499-509.
[37] Kosty J, Lu F, Kupp R, et al. Harnessing OLIG2 function in tumorigenicity and plasticity to target malignant gliomas. Cell Cycle Georget Tex 2017;16:1654-60.
[38] Lu F, Chen Y, Zhao C, et al. Olig2-dependent reciprocal shift in PDGF and EGF receptor signaling regulates tumor phenotype and mitotic growth in malignant glioma. Cancer Cell 2016;29:669-83.
[39] Kupp R, Shtayer L, Tien A-C, et al. Lineage-restricted OLIG2-RTK signaling governs the molecular subtype of glioma stem-like cells. Cell Rep 2016;16:2838-45.